

# Performance Prediction of MemS Based Resistojet Thruster Through CFD

Syed Sheraz Ali <sup>a</sup>, Dr. Nauman Qureshi <sup>b</sup> and Captain Dr. Shafiq ur Rehman <sup>c</sup>

**Abstract**—The advent of MEMS has shifted the trend from bulkier satellites to pico or nano satellites, owing to their low manufacturing and launch cost. This project involves the numerical modeling (CFD), simulation and performance prediction of proposed micro-resistojet thruster configuration. After the validation of our numerical CFD methods and results with available numerical and experimental data, a parametric study has been conducted. The effects of change of mass flow rate of the working fluid ( $N_2$  gas in this case) and the heater temperature on Thrust; Specific Impulse ( $I_{sp}$ ) and viscous subsonic layer thickness has also been investigated. It has been developed that optimum results are found for mass flow rate of 1.2 mg/s and at heater temperature of 500°C.

**Index Terms**— CFD, micro-nozzle, nano-satellites, thrust

## I. INTRODUCTION

Low weighted and small sized devices have attracted tons of people around the globe. When it comes to laptops, computers and cellphones, the smaller the better. The satellites show is now moved down to shrink sizes. They are smaller, take less time to design and build, with low launch cost, low thrust production and low power consumption. Above all, they weigh less (pico satellites with less than 1kg and nano satellites with less than 10kg). These subsystems involves MEMS based micro-propulsion systems, employed in micro-thrusters. They are used to simplify the operations by reducing size and increasing the output. Resistojet are then implanted in MEMS to provide thrust in various applications. This surprisingly tiny size, nanosats possess unique propulsion system and ability to deliver very low thrust, impulse for attitude control and orbital maneuvering [2].

Fig. 1 shows their movement, followed by the principle of thrust – an equal but opposite ejective force, obtained from resistojet [1].

This work was supported in part by Suparco, Shaheen foundation and PNEC NUST.

Engr. Syed Sheraz Ali is working as a lecturer in DHA Suffa university, Karachi, Pakistan (Phone: 0345-535-2014; e-mail: [stunninghp@gmail.com](mailto:stunninghp@gmail.com)).

Dr. Nauman Qureshi is currently working as Head of Department, Mechanical engineering, in DHA Suffa University., Karachi Pakistan. (E-mail: [mnuamanqureshi@gmail.com](mailto:mnuamanqureshi@gmail.com)).

Captain Dr. Shafiq ur Rehman was working as a Dean (ES), in Pakistan Naval Engineering College, NUST, Karachi Pakistan. Currently, he is posted to Islamabad, Pakistan in naval HQ. (E-mail: [shafiqpn1@gmail.com](mailto:shafiqpn1@gmail.com)).

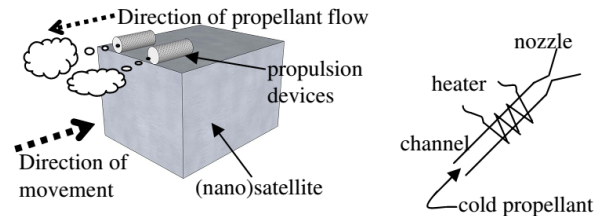


Fig. 1 Conceptual sketch of cubesat.

The development is ongoing on satellites of class nano (mass 1 – 10 kg), pico (0.1 – 1 kg) and femto satellites (less than 100g). It is necessary to miniaturize, to meet the global need of microspacecraft projects [3].

To test their performances, CFD methods are generally used. In this report, the prediction performance of MEMS based resistojet thruster is presented using parameters: Thrust, Specific Impulse and Subsonic Layer. The investigation is based on variable mass flow rate of Nitrogen gas, as it passed through the heater section to different heater temperatures.

### A. Description of Micro-thruster

MEMS stand for Micro Electro Mechanical Systems that range from few micrometers to millimeters. It contains mechanical and electrical components (Micro sensors, Micro actuators, Micro structures), all integrated on single silicon chip. MEMS are one of the most important revolutionary innovations in the field of electronic market. Nowadays, the precision is desired for maneuvering and for that micronozzles of few hundred microns or below are fabricated.

They are used to simplify the operations by reducing size and increasing the output. Resistojet are then implanted in MEMS to provide thrust in various applications. This surprisingly tiny size, nanosats possess unique propulsion system and ability to deliver very low thrust and impulse for attitude control and orbital maneuvering [2].

They are tiny, light, low power, and cost effective fabricated device [4]. It is therefore, not deter by shock and radiations. The current trend for such device tends towards micro-thrusters, for defense purpose in space industry. The reason behind is to get high power to weight ratio, with low cost over manufacturing and maintenance. Below are listed flow through micro-nozzles in the fields of automobile, aerospace, biomedical, defense and electronics [5] as shown in Fig. 2.



Fig. 2 MEMS application.[5]

MEMS are developed as an integrated micro satellite with the digital micro propulsion. This sort of space operation is used for orbiting mission. Its stabilization required lower thrust (0.1 – 10 mN). This is achieved with cold gas thruster. The thrust is generated with a high pressure gas expands through a nozzle. These thrusters have small specific impulse, normally 70s. One of its essential component is that nozzle needs to be microminiaturized [6].

### B. Resistojet

Resistojet is a propulsion device, which heats the propellant as it passes through a heated section (heat exchanger) and allows it to expand through a downstream nozzle. The description is shown in Fig. 3:

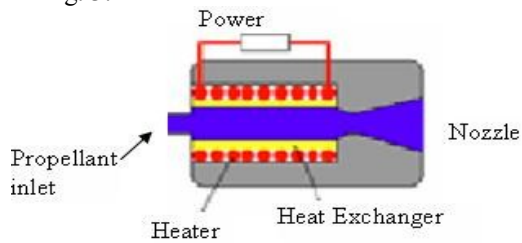


Fig. 3 Resistojet working principle.

It is useful to heat the propellant before it leaves the nozzle, to get characteristic velocity. Through force convection, propellant is heated with a heater element. It is best suitable for small  $\Delta V$  missions ranging upto 200m/s. It has high thrust to power ratio and good specific impulse (100 – 200s). It is therefore, suitable for altitude control operations for nano-satellites.

### C. Working

A converging diverging nozzle is applied for such kind of flows. They have to provide thrust by changing the gas molecules into kinetic energy. At first section, the flow is subsonic due to low acceleration. The sonic conditions are met at nozzle throat. However, the divergent flow in downstream further accelerates the flow and a supersonic expansion occurs at the last stage. The subsonic viscous layer formation due to low Reynolds number at micronozzle divergent area reduces thrust production.

The nitrogen gas is injected from pressurized bottle, through mass flow controller (MFC) that can deliver various mass

flows. The nozzle inlet pressure ( $P_c$ ) which is responsible for mass flow rate and the thrust, is determined from difference of system pressure  $P_s$  and pressure drop  $\Delta P$  (inherited in device) [1].

### D. Measuring Parameters

**Thrust, F** is opposite reaction force, measured in N can be found from (1). Here  $\dot{m}$  is mass flow rate, P is pressure, V is axial velocity and A is Area. While subscripts 'e' and 'o' are for exit and ambient respectively.

$$F = \dot{m}_e V_e - \dot{m}_o V_o + (P_e - P_o) A_e \quad (1)$$

**Specific impulse,  $I_{sp}$**  is measure of efficiency of rockets and jets (seconds). It is found as below:

$$I_{sp} = F / \dot{m} g \quad (2)$$

The **subsonic viscous area** is simply the ratio of subsonic layer at nozzle exit,  $A_s$  to nozzle outlet area,  $A_o$  as shown in (3)

$$\text{Subsonic Area Ratio} = A_s / A_o \quad (3)$$

### E. Our Design

In our MEMS resistojet thruster, prediction is based on the model proposed by [1] as shown in Fig. 4. The dimension of micro-thruster is (26 x 5 x 1 mm).  $N_2$  gas, of different mass flow rates, is used as a cold thruster, which is passed through the inlet manifold to the heater section. Afterwards, variable heater temperatures are to heat the mono-propellant before it enters the converging diverging nozzle. The pressure is kept 5 bar for the flow of gas, in the range of 0.35 ~ 0.85 mg/sec.

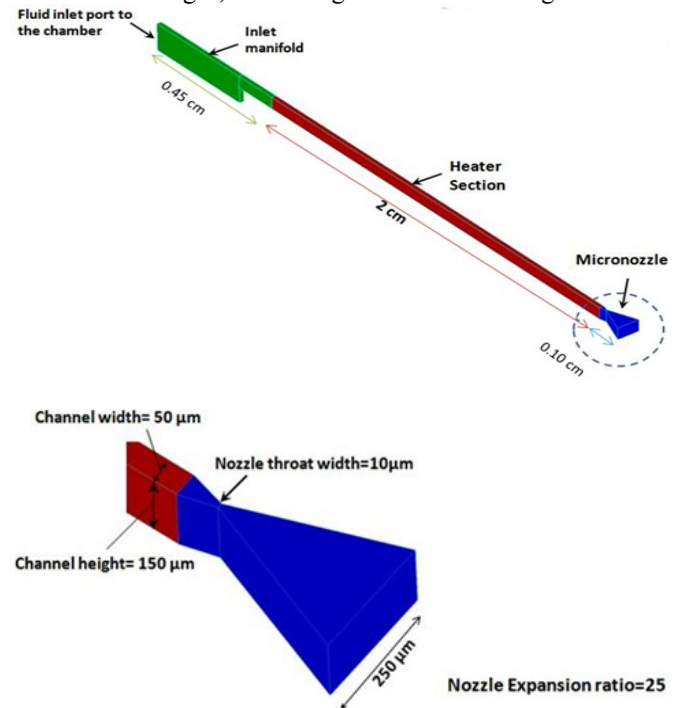


Fig. 4 Design of MEMS resistojet thruster. (a) Overall geometry of microthruster including resistojet (b) Focus on micronozzle

### F. State of Methodology

The literature review has been carefully undertaken, verifying the procedures. Ref [1] data is close to our proposed geometry and we have to cover that aspect accordingly. The preprocessing involves; meshed geometry exported from Gridgen v15.0 to ANSYS Fluent v14.0 for simulations. Grid independence study is carried out to verify the optimum grid. Eventually, numerical simulations are carried out under prescribed boundary conditions and schemes. The post processing involves determining the three performance parameters for micro thrusters: Thrust, Subsonic Layer Area and Specific Impulse. The results are then compared to above mentioned paper results and validated. The improved results are further processed to SETC for fabrication.

The viscous subsonic layer formation in micro nozzle was first investigated by [6]. They acknowledged that the viscous layer formation diminishes the flow and increases thrust loss [7]. Ref [8] said that the flow in microscale nozzles are viscous supersonic flow ( $Re < 1000$ ,  $1 < Ma < 5$ ). This special design of micronozzle enhances the efficiency of microthruster. It can reduce costs, economical fuel consumption and increase satellite life span. This reduce tank volume and hence weight.

The main factor of any micro propulsion system is converging diverging supersonic section that converts pressure and thermal energy of propellant into thrust. The viscous flow owing to low Reynolds number can substantially affect the micro nozzle performance. The subsonic layer can become thick enough to halt the bulk flow and reduces the thrust production, hence efficiency as discussed by [9].

According to [10] the subsonic flow can be diminishing by two ways: Increase the divergence angle or to build a deep micronozzle. The former method can cause geometrical losses at larger angle, due to transverse velocity at nozzle outlet.

Ref [9] mentioned the advancement in fabrication in micro and nano level has put bell shaped expander under consideration. It nearly recovers axial flow at expander exit and shortens the viscous boundary layer formation. Hydrogen peroxide, monopropellant, is used as working fluid. The advantage of monopropellant lies in its simplicity to use and relatively high energy density. Reynolds number can be found by:

$$Re = \frac{mL}{\mu A} \quad (4)$$

Where  $m$  is mass flow rate,  $L$  is characteristic length,  $\mu$  is dynamic viscosity and  $A$  is cross sectional area. He concluded that that reducing the length of bell nozzle reduces the viscous subsonic layer.

## II. MODELING

The fluid flow in the micro-channel and micro-nozzle is considered to be as continuum and the flow behavior is modeled using Navier Stokes equations.

### A. Continuum Approach

Generally, the fluid is treated as continuum as it is difficult to calculate the discrete particles. Continuum means 'range', 'band' or 'variety'. In this method, the study is concerned dealing with materials that are modeled continuous rather than discrete particles. The particles that are solids, liquids or gases

are thought to be continuously distributed and have no empty space [12].

The body is divided into infinitesimal elements, having the same property as of entire unit cell. Macroscopic variables like temperature are calculated instead of microscopic values such as molecular velocity. It is an idealization where the matter is described continuous within matter. While in continuum approach, the fluid properties are expressed as continuous function of space that is temperature, density, viscosity etc.

### B. Knudsen Number

In fluids, it is used excessively to determine the continuity approximation. A continuum model is defined well with the help of molecular density. Mean free path between molecules are characterized by mean free path. It is obtained by average distance of molecules between two successive collisions [13].

#### Mathematical Form

It is a dimensionless number, ratio of mean free path,  $\lambda$  and the characteristic length,  $L$ .

$$Kn = \lambda/L \quad (5)$$

Knudsen number is the relation to indicate the flow rarefaction. For Knudsen number less than 0.01, we adopt the continuum approach, neglecting any rarefaction and hence using Navier Stokes equation. While, if  $Kn > 0.01$  the molecular level study is prompted, using DSMC (Direct Simulation Monte Carlo) and Molecular Dynamics (MD) to solve equations. This technique is used by tracking each particle with its position, velocity and internal energy (13). The Knudsen number only holds viable under the value of 0.01. Knudsen # is also described in terms of ratio of Mach number and Reynolds number (13):

$$Kn = \sqrt{\gamma\pi/2} \frac{M}{Re} \quad (6)$$

### C. Criteria

Knudsen number categorized into different regimes (11) as shown in TABLE :

TABLE I  
KNUDSEN NUMBER VERIFICATION

Knudsen Number	Comments
(0.01 < Kn < 0.1)	Slip flow (continuum flow)
(0.1 < Kn < 1)	Transition Flow
Kn > 0.01	No continuum exists
(Kn > 10)	Free molecule flow

In our case, the Knudsen number ( $Kn = 0.0002$ ) comes to be in continuum region.

### D. Governing Equations

The fluid flow governed by three fundamental equations: Continuity, Energy and Navier Stokes.

### Continuity Equation

The Reynold number describes our model to be **laminar flow**. For incompressible steady state flow, the continuity equations becomes

$$\frac{\partial \rho}{\partial t} + \rho \frac{\partial u}{\partial x} + \rho \frac{\partial v}{\partial y} + \rho \frac{\partial w}{\partial z} = 0 \quad (7)$$

### Navier Stokes Equation (Momentum Equations)

Navier Stokes equations also known as momentum equations, derived from 2<sup>nd</sup> law of Newton. It is defined by summing all forces in a direction opposite to the change in momentum. It can be body or surface forces. They are shown as below:

$$\rho \left[ \frac{\partial v_x}{\partial t} + v_x \frac{\partial v_x}{\partial x} + v_y \frac{\partial v_x}{\partial y} + v_z \frac{\partial v_x}{\partial z} \right] = \rho g \vec{i} - \frac{\partial P}{\partial x} + \mu \left[ \frac{\partial^2 v_x}{\partial x^2} + \frac{\partial^2 v_x}{\partial y^2} + \frac{\partial^2 v_x}{\partial z^2} \right] \quad (8)$$

$$\rho \left[ \frac{\partial v_y}{\partial t} + v_x \frac{\partial v_y}{\partial x} + v_y \frac{\partial v_y}{\partial y} + v_z \frac{\partial v_y}{\partial z} \right] = \rho g \vec{j} - \frac{\partial P}{\partial y} + \mu \left[ \frac{\partial^2 v_y}{\partial x^2} + \frac{\partial^2 v_y}{\partial y^2} + \frac{\partial^2 v_y}{\partial z^2} \right] \quad (9)$$

$$\rho \left[ \frac{\partial v_z}{\partial t} + v_x \frac{\partial v_z}{\partial x} + v_y \frac{\partial v_z}{\partial y} + v_z \frac{\partial v_z}{\partial z} \right] = \rho g \vec{k} - \frac{\partial P}{\partial z} + \mu \left[ \frac{\partial^2 v_z}{\partial x^2} + \frac{\partial^2 v_z}{\partial y^2} + \frac{\partial^2 v_z}{\partial z^2} \right] \quad (10)$$

### Energy Equation

Total energy is combination of kinetic energy, potential energy and thermal energy. It can be written in compact form:

$$\rho(\nabla \cdot \mathbf{V}) = \nabla \cdot (k \nabla T) + \Phi \quad (11)$$

Here, 'k' is thermal conductivity and  $\Phi$  is dissipation function.

### E. CFD Analysis

To perform a CFD analysis, the flow domain has to be discretized. This discretization is done by surface grid/mesh in 2D space and by polyhedrons in case of 3D computational domain. The finite volume numerical analysis methods are then applied on the discretized domain and solution is sought using iterative methods till the desired convergence level is achieved.

In this work, AutoCAD is used for modeling the micro-thruster geometry. Gridgen v15.0 is used for meshing; setting boundary conditions and exporting ANSYS Fluent 14.0 case file for simulation work. Post processing is carried out in ANSYS Fluent 14.0.

The mathematical model conforms to CFD model, as the flow is laminar and incompressible. Hence we can use incompressible continuity equation in this case. Also the overall flow in the microthruster is not exceeding the Reynolds number beyond the threshold of Laminar flow. Hence the simulations are not carried for turbulent flow, but for laminar flow.

While the flow is 2D, so the 3D Navier Stroke's equation is applied with Nitrogen gas flowing in axial direction only. The energy equation is also used, with constant values of thermal conductivity and viscosity.

### Geometry

The geometry has been made on AutoCAD. It is simple 3D micro jet nozzle. The geometry consists of three sections as shown in Fig. 5. The figure further elaborates the dimension of microzzle, with respect to its height, width and throat area.

-1- Inlet manifold -2- Heater Section -3- Micro Nozzle

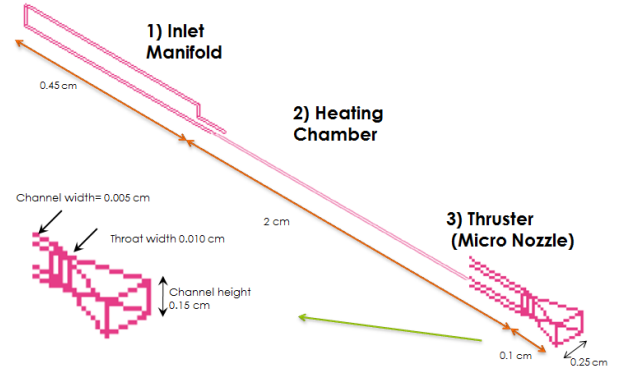


Fig. 5 Dimension distribution of model design.

### Meshing

For meshing, Gridgen v15.0 has been used. The mesh is generated in three steps: creating connectors, developing domains and building blocks.

After importing geometry (database), connectors were made with domains and blocks successively. The geometry consists of structured hexahedral mesh for 3D and structured quadrilateral mesh for 2D planar.

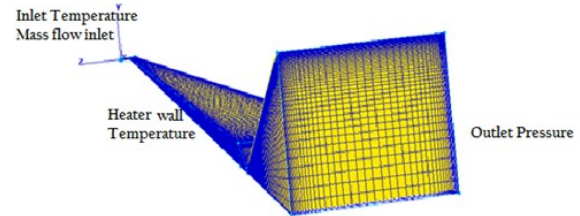


Fig. 6 shows microthruster mesh.

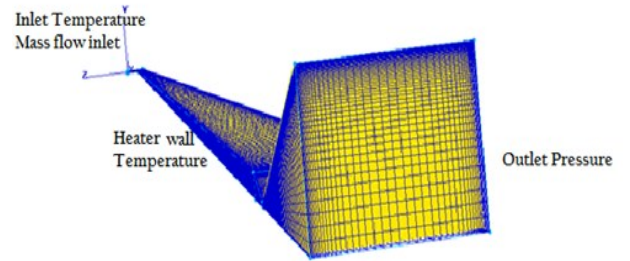


Fig. 6 Orthogonal view of MEMS microthruster grid.

### Boundary Conditions

The mesh is set with boundary conditions at the inlet, heater and outlet. No slip condition is used at the wall. Taking advantage of the symmetry and to reduce computational cost, half geometry is modeled with xz as symmetry plane. Boundary conditions are shown in TABLE II.

TABLE II  
BOUNDARY CONDITIONS

Boundary Conditions			
Inlet temperature	23°C	Inlet mass flow rate	0.35, 0.85, 1.2 (mg/s)

Outlet pressure	50 Pa	Heater wall temperature, $T_h$	100 °C, 300 °C, 400 °C, 500 °C
-----------------	-------	--------------------------------	--------------------------------

### Simulation Work

It is then ready to be imported as .cas file in fluent, which can be ready to execute in fluent software. Pressure based solver is implemented, as flow is low speed (laminar). Hence, 12 cases have to be run in all, four working fluid temperatures against each of the three mass flow rates as shown below in TABLE III.

TABLE III  
SIMULATION CASES

Mass Flow Rate (mg/s)	Heater Temperature (°C)			
0.35	100	300	400	500
0.85				
1.2				

In ANSYS FLUENT, the properties of the working fluid (nitrogen) are defined in TABLE . These values are predefined in ANSYS Fluent:

TABLE IV  
PROPERTIES OF NITROGEN GAS USED FOR COMPUTATION

Property	Units	Method	Value
Density	kg/m <sup>3</sup>	Ideal Gas	variable
Cp (specific heat)	J/kg-K	Piecewise-Polynomial	variable
Thermal conductivity	W/m-K	Kinetic Theory	variable
Viscosity	kg/m-s	Sutherland Law	variable
Molecular weight	Kg/k-mol	Constant	28.0134

The simulation is performed in ANSYS Fluent V14.0 with 3D, laminar and double precision. The nitrogen gas has been selected as working fluid is then set different properties. The 3D steady laminar simulations have been performed using ANSYS Fluent. A second order upwind has been used for the governing equations. SIMPLE scheme has been employed for pressure velocity coupling. Under relaxations factors are shown as below in TABLE V:

TABLE V  
UNDER-RELAXATION FACTORS USED IN FLUENT

Under-Relation Factors	Values
Pressure	0.1
Momentum	0.1
Density	0.1
Energy	0.1

### Convergence Criteria

The simulations have been run till following criteria met: Residuals less than  $10^{-10}$  are achieved; the net mass flow rate drops four order of magnitudes in comparison with inlet mass flow rate and no changing in thrust value. When all these conditions are met, the solution is considered to be converged.

### Grid Independence Study

To correctly investigate the problem of micro thruster and predict its result properly, simulations have been performed on

three separate grids G1, G2 and G3. These have grid sizes 797808, 1260868 and 1334000 quadrilateral cells respectively. Fig. 7 shows the 2<sup>nd</sup> grid (G2):

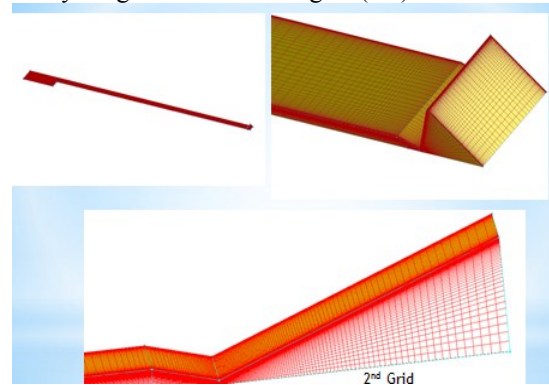


Fig. 7 Second Grid G2.

### Grid independence results

The result sheet for a micro-thruster (

TABLE VI), with N<sub>2</sub> gas flowing at 0.85 mg/s with heater temperature of 300 °C for three different grids is as followings:

TABLE VI  
GRID INDEPENDENT STUDY POST PROCESSING RESULTS.

Mesh size	Thrust (mN)	Isp (s)	Subsonic Area, As (%)
0.7 M (G1)	0.726	87.15	22.12
1.2 M (G2)	0.719	86.97	21.96
1.33 M (G3)	0.709	85.09	21.67

It is noted that the grid sizing does not have sizable impact on results. However, the finest mesh G3 is accounted for further simulation results, for better result. The parameter trends for three grids are shown below in Fig. 8, Fig. 9 and Fig. 10.

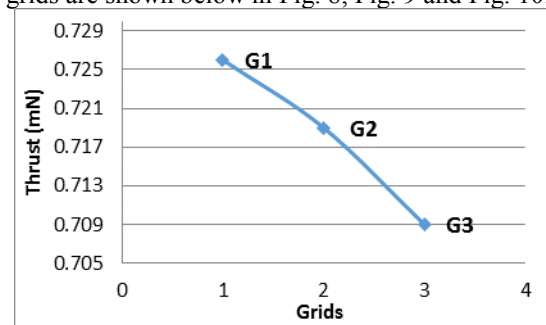


Fig. 8 Grid independence study for thrust.

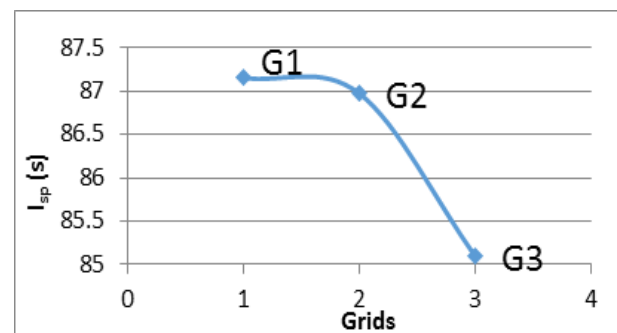


Fig. 9 Grid independence study for specific impulse.

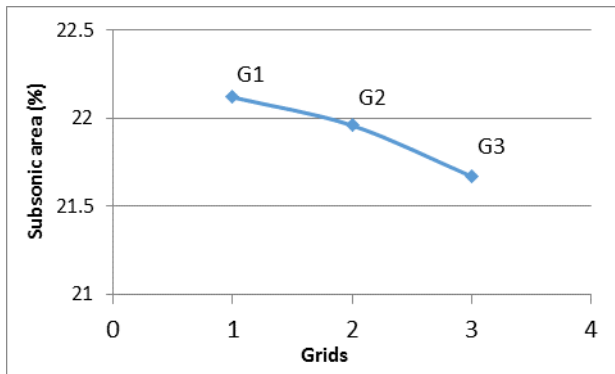


Fig. 10 Grid independence Study for subsonic area.

Furthermore, the Mach contours confirm the grid independence study from Fig. 11.

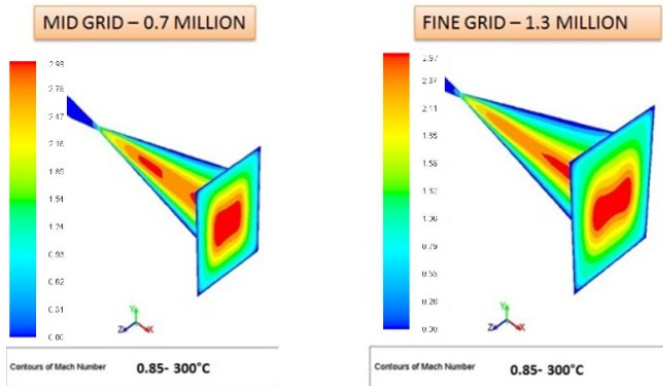


Fig. 11 Grid independent CFD results (Mach contours).

### III. SIMULATIONS RESULTS

After selecting the fine grid of 1.33 million cells, in total 12 cases are run for four working fluid temperatures with three mass flow rates each. The processed results for subsonic area, thrust and specific impulse are listed in TABLE VII:

TABLE VII

POST-PROCESSED RESULTS SUMMARY

Temperature (°C)	Subsonic area (%)	Thrust (mN)	$I_{sp}$ (s)
<b><math>\dot{m} = 0.35</math> mg/s</b>			
100	26.31	0.238	69.46
300	28.71	0.285	82.97
400	29.55	0.305	88.84
500	30.24	0.324	94.36
<b><math>\dot{m} = 0.85</math> mg/s</b>			
100	22.93	0.594	71.28
300	25.30	0.709	85.09
400	24.10	0.775	92.96
500	23.45	0.838	100.59
<b><math>\dot{m} = 1.2</math> mg/s</b>			
100	20.48	0.848	72.04
300	20.64	1.042	88.54
400	22.33	1.112	94.48

500	22.11	1.189	101.02
-----	-------	-------	--------

#### A. Subsonic area

Generally, the subsonic viscous area ratio decreases with the increase in mass flow rates. For mass flow rate of 0.35 mg/s, the area ratio increases slightly with heater temperature. Whereas in case of 0.85 mg/s and 1.2 mg/s, no specific trend is found as shown in Fig. 12. It will be explained later.

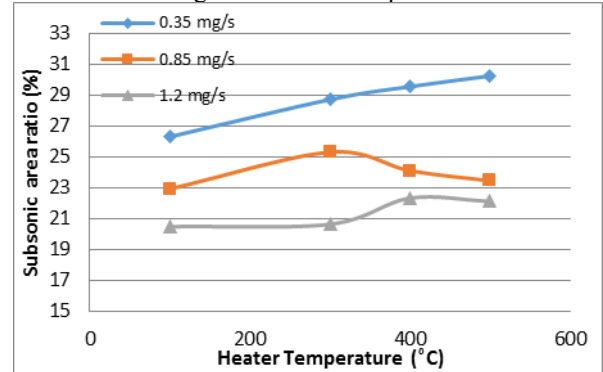


Fig. 12 Subsonic viscous area result.

#### B. Thrust

The thrust achieved at the nozzle exit, is increased with increase in mass flow rate as well as with increase in heater temperature. For particular heater temperature the increase in thrust is mainly due to increase in mass flow rates. For same mass flow rate the increase in thrust is mainly due to increase in momentum thrust as shown in Fig. 13.

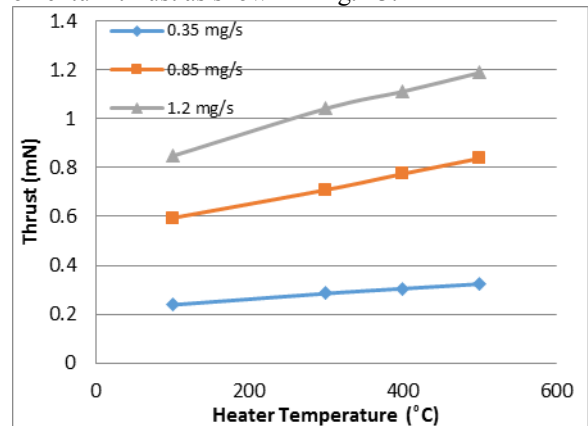


Fig. 13 Thrust for all mass flow rates.

#### C. Specific impulse ( $I_{sp}$ )

Fig. 14 displays the trends of specific impulse also like thrust, since it is directly derived from thrust.

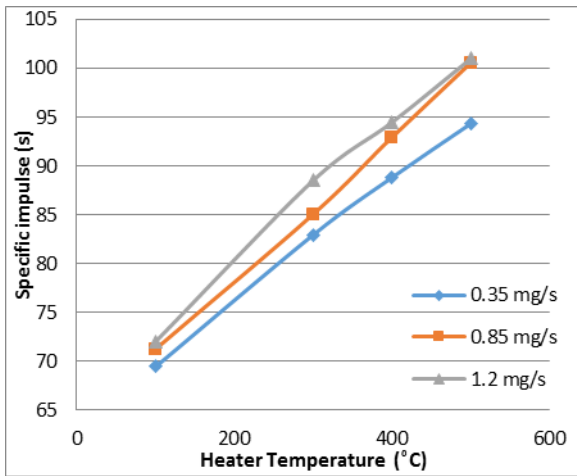


Fig. 14 Specific impulse for all mass flow rates.

**D. Mach contours at micro-nozzle exit**

The Mach number contours and subsonic viscous layer for mass flow rate of 0.35 mg/s are shown below in Fig. 15 and Fig. 16.

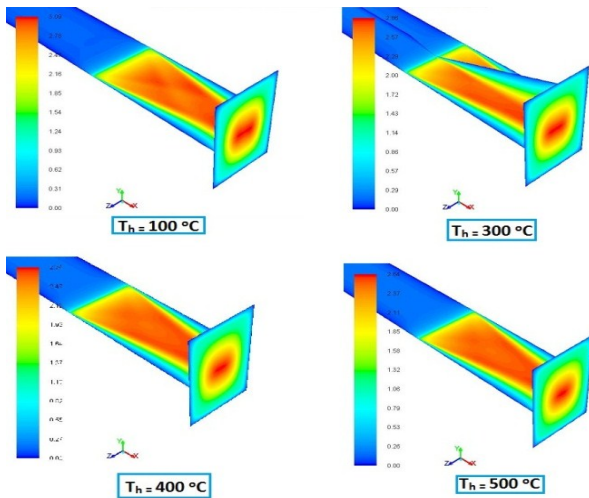


Fig. 15 Mach results for 0.35 mg/s.

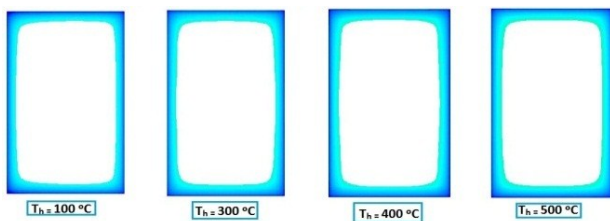


Fig. 16 Subsonic viscous layer results for 0.35 mg/s.

It has been observed from the Mach contours (in Fig. 15 and Fig. 16), that the viscous subsonic layer is developed across the walls of micronozzle. This viscous subsonic layer formation reduces the efficiency (thrust formation) of thruster, as it does not allow the full thrust as should have been produced which is desired. The Mach number also indicated the supersonic formation in the middle and it is decreasing from the center to the corner of the wall. The temperature which is increased from inlet manifold from room temperature

to heater temperature, and it is further throttled at the throat of micronozzle.

The above Fig. 16 indicates that the specific impulse  $I_{sp}$  of the micronozzle for flow of 0.35 mg/s increases as the heater temperature increases in the micronozzle. The value of thrust is increasing, with rise in heater temperature. Therefore, it can be seen that heater temperature is important parameter in controlling the thrust effect of micronozzle.

The same result can be deduced for mass flow rate of 0.85 mg/s. The thrust  $F$  and specific impulse  $I_{sp}$  has increasing trend with the rise of heater temperature. In addition to heater temperature, mass flow rate also alter the thrust production at the nozzle outlet.  $I_{sp}$ , the efficiency criteria, is also increasing with increase in inlet mass flow rate. The losses in the form of subsonic viscous layer, that is formed at the walls of diverging portion of micronozzle, is condensed to permit more thrust produced at the end of micronozzle. In Fig. 17, Mach contour formation (for  $\dot{m} = 0.85$  mg/s,  $T_h = 300$  °C) is shown to understand the viscous layer formation, from throat to exit of micronozzle.

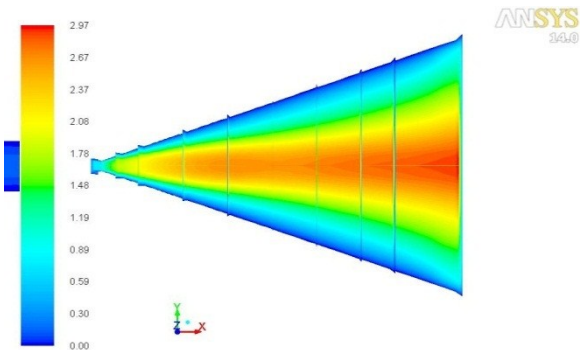


Fig. 17 Mach number ranging from throat to exit of micronozzle.

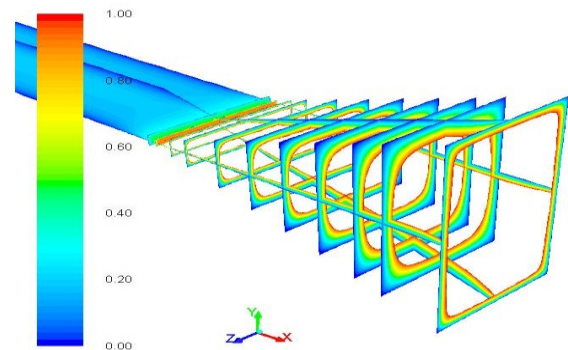


Fig. 18 Viscous subsonic layer growth from micronozzle throat to exit.

In above Fig. 18, the trend is shown for viscous subsonic layer formation (for  $\dot{m} = 0.85$  mg/s,  $T_h = 300$ °C). It can be seen that the subsonic viscous layer formed at nozzle throat, which first increases gradually up to 90% of divergent length and then decreases as it reaches the exit. It can be deduced, herewith, that losses are reduced with increase in the length of diverging section.

### E. Result Comparison for Nozzle Inlet Stagnation Pressure

Moreover, our results can be validated by comparing the experimental results (1) for nozzle inlet stagnation pressure. The validation of model depends on error falling less than 10%, so that it can be considered acceptable for further evaluation. In TABLE VIII and IX, various heater temperatures for mass flow rates ( $0.35 \text{ mg/s}$  and  $0.85 \text{ mg/s}$ ) are shown against nozzle inlet pressure,  $P_c$ . The columns comprise, from left to right are as following: Heater Temperature ( $T_h$ ), the project simulated nozzle inlet pressure ( $P_c$ ), from (1) experimental data system pressure ( $P_s$ ) and percentage difference.

TABLE VIII  
PRESSURE DATA TABLE FOR  $M = 0.35 \text{ MG/S}$

Heater Temperature $T_h$ [°C]	Project CFD Results Nozzle Inlet Pressure, $P_c$ [Bar]	Experimental Results System Pressure, $P_s$ [Bar]	Percentage difference / Error $\frac{P_c - P_s}{P_c} \times 100$ [%]
100	1.99	1.81	9.04
300	2.41	2.20	8.71
400	2.58	2.39	7.36
500	2.80	2.62	6.43

TABLE IX  
PRESSURE DATA TABLE FOR  $\dot{m} = 0.85 \text{ MG/S}$

Heater Temperature $T_h$ [°C]	Project CFD Results Nozzle Inlet Pressure, $P_c$ [Bar]	Experimental Results System Pressure, $P_s$ [Bar]	Percentage difference / Error $\frac{P_c - P_s}{P_c} \times 100$ [%]
100	3.64	3.94	8.24
300	4.3	4.63	7.67
400	4.71	5.05	7.22
500	4.88	5.2	6.56

The results are compared as shown in Fig. 19 (for  $\dot{m} = 0.35 \text{ mg/s}$ ) and Fig. 20.

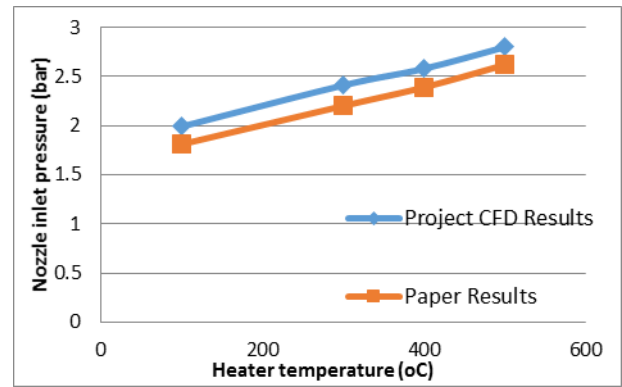


Fig. 19 validating nozzle inlet pressure results for  $0.35 \text{ mg/s}$ .

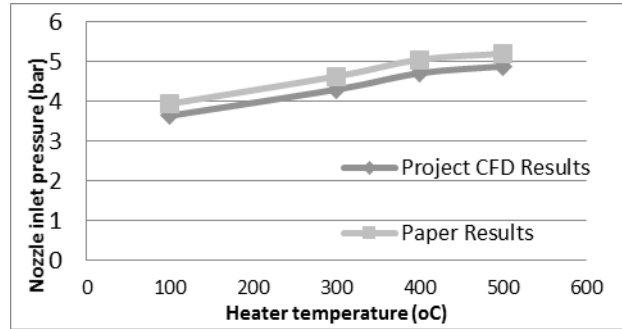


Fig. 20 Validating nozzle inlet pressure results for  $0.85 \text{ mg/s}$ .

### F. Thrust Verification

In order to validate results, the thrust values calculated in the project are matched with the thrust values calculated by Mihailovic et al. (1) in his paper. He presented the thrust values for set mass flow rates ( $0.35 \text{ mg/s}$ ,  $0.85 \text{ mg/s}$  and  $1.2 \text{ mg/s}$ ). The result values are shown as below in Fig. 21:

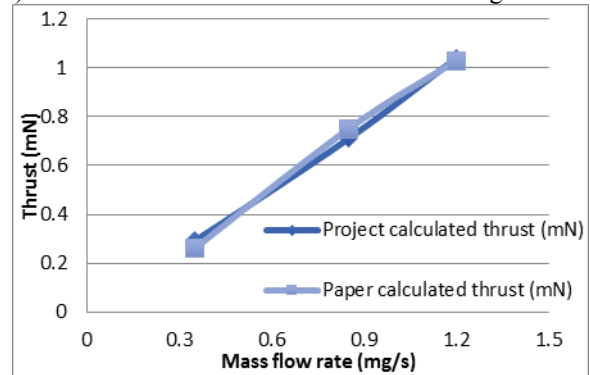


Fig. 21 Thrust comparison.

### G. Knudsen Number Verification

The simulations ran were on the theoretical assumption from given values of throat region of thruster, that it is with continuum regime. The above said approach is verified once we run it for different temperatures. Knudsen number can be found by using eq. (6). The values are shown in TABLE X.

TABLE X  
KNUDSEN NUMBER AT THROAT OF MICRONOZZLE

Mass flow rate (mg/s)	0.35 mg/s	0.85 mg/s	1.2 mg/s
Temperature (°C)	Knudsen Number		
100	0.0004	0.0004	0.0004
300	0.0003	0.0003	0.0003
400	0.0003	0.0003	0.0003
500	0.0003	0.0002	0.0002

#### IV. CONCLUSION

Numerical modeling and simulation of a micro resistojet thruster has been performed in this work. A total of 12 cases for three mass flow rates of working fluid ( $N_2$ ) and four heater temperatures, each are simulated. The results are computed in terms of subsonic viscous area, thrust and specific impulse. The results on thrust for three mass flow rates at heater temperature of  $300^\circ\text{C}$  are compared with the results (1). Comparison of nozzle inlet chamber pressure is done with the system pressure determined indirectly in (1). Following conclusions can be drawn from the performed simulations:

1. The assumption of considering the fluid as continuum has been found to be correct as Knudsen numbers is found to be less than 0.0005 for all the cases, at throat of micronozzle.
2. The subsonic viscous layer growth is successfully captured for all the cases. For mass flow rate of 0.35 mg/s, the viscous subsonic area at the micronozzle exit has slight increasing trend with increasing heater temperature. For the rest of the two mass flow rates no specific trend is observed. The subsonic viscous area varies from 20% to 30%. It is minimum for mass flow rate 1.2 mg/s at  $100^\circ\text{C}$  and maximum for mass flow rate 0.35 mg/s at  $500^\circ\text{C}$ .
3. The micronozzle thrust is found to vary from 0.2mN to 1.2 mN for the cases studied. For same mass flow rate the thrust increased with the increase of heater temperature. This is due to the increase in momentum thrust as the nozzle exit velocity increases. For same heater temperature the increase in thrust with the increase of mass flow rate is simply due to the increase in working fluid mass flow rate.
4. The  $I_{sp}$  trends are same as that of thrust as it is directly derived from thrust. The  $I_{sp}$  varied from 69s to 101s for the studied cases. The lowest value corresponds to the lowest mass flow rate and the lowest heater temperature. The highest  $I_{sp}$  is achieved for mass flow rate of 1.2 mg/s and heater temperature of  $500^\circ\text{C}$ .
5. The nozzle inlet chamber pressure is compared with the experimentally derived system pressure (1). The difference is found to be within 10%.

6. The thrust values for three mass flow rates at heater temperature of  $300^\circ\text{C}$  are also compared with analytical results (1). The thrust values also lie within 10%.

7. The results will help in further designing and manufacturing of micro thruster. It will help the designer to deduce, that with change in gas mass flow rate, heater temperature or dimension of micronozzle, we can alter the performance (specific impulse, thrust and subsonic layer) of micronozzle.

Thus, encouraging the need of any developing country for its optimum production.

#### A. Future Work

The above results obtained from the simulations of micronozzle, resulted in modification of its application in the field of space and technology. The variation of mass flow and heater temperature of the Nitrogen gas used, can alter the performance of the micronozzle. The thrust, specific impulse and subsonic area changes with the change in above mentioned parameters.

On the other hands, if one desired to use different gas like Argon or Helium, with constant or variable temperature will obtain the same pattern.

The CFD modeled results will help defense industries to enhance their capabilities in space program. After successful product from designing the working of micronozzle will further help the manufacturer to fabricate small scale micronozzle for thrust purpose.

The key objective of the task to do so is to enhance the use of technology with thermo fluids. It will further help any developing country in several applications. Of which range from experimental setup to explore mission, geostationary operations to espionage work.

#### REFERENCES

- [1] M. Mihailovic, T.V. Mathew, J.F. Creemer et al. (2011). Mems silicon-based resistojet micro-thruster for attitude control of nano-satellites. Delft Netherland.
- [2] W.F. Louisos, A.A. Alexeenko and D.L. Hitt and A. Zilić. (2008). Design considerations for supersonic micronozzles. Vermont USA.
- [3] Fleeter, R. (2000). *The Logic of Microspace*. Microcosm Press and Kluwer Academic Publisher.
- [4] H.R. Shea (2009). MEMS for pico- to micro-satellites. Switzerland Rue Droz, CP 526 Neuchatel.
- [5] An Introduction to MEMS (Micro-Electromechanical Systems), Loughborough University, PRIME Faraday Partnership, ISBN 1-84402-020-7, January 2002.
- [6] Liu, M. (2002). *Micropropulsion for space – a survey of memsbased micro thrusters and their solid propellant technology*. Hefei, China: University of Science and Technology of China.
- [7] R.L. Bayt and K.S. Breuer (1998). *Viscous Effects in Supersonic MEMS-based Micronozzles*. Anaheim, CA: Proc. 3rd ASME Micro fluids Symp.
- [8] Bayt, R. (1999). *Analysis, fabrication and testing of a MEMS fabricated micronozzles*. MIT, Cambridge .

- [9] Jason M. Pearl, William F. Louisos and Darren L. Hitt (2010). *Numerical Design of Plug Nozzles for Micropropulsion Applications*. USA: University of Vermont.
- [10] Ahsan Choudhuri, Benjamin Baird, S. Gollahalli, and Steven Schneider (2001). *"Effects of geometry and ambient pressure on micronozzle flow"*, 37th Joint Propulsion Conference Reed, B. (2003). *Decomposing solid micropropulsion nozzle performance issues*. Reno, Nevada : 41<sup>st</sup> AIAA.
- [11] W.F.Louisos and D.L.Hitt. (2005). Optimal expansion angle for viscous supersonic flow in 2-D micro nozzles. *35th AIAA Fluid Dynamics Conference and Exhibit*. Ontario Canada: AIAA.
- [12] Louisos, W.and Hitt, D.L (2009). *Numerical Simulations of Viscous Flow in 3D Supersonic Bell Micronozzles*. Vermont: 47<sup>th</sup> AIAA conference.
- [13] Morinishi, K. (2006). A Continuum/ Kinetic Hybrid approach for multi scale flow simulation. (p. 18). Kyoto, Japan: ECCOMAS CFD.
- [14] Pitakarnnop, A. J. (2012). *Rarefied gas flow in pressure and vacuum measurements*. Busan, Republic of Korea: National Institute of Metrology, Prathumthani, Thailand.
- [15] Liu. M, Zhang.X and Zhang.jee G (July 2006). *Study on micronozzle flow and propulsion performance using DSMC and continuum methods*. University of Science and Technology of China.